

The Evolving Role of Cardiovascular Magnetic Resonance Imaging in the Evaluation of Systemic Amyloidosis

Sanjay M Banypersad

Royal Blackburn Hospital, Blackburn, UK.

Magnetic Resonance Insights
Volume 12: 1–10
© The Author(s) 2019
Article reuse guidelines:
sagepub.com/journals-permissions
DOI: 10.1177/1178623X19843519



ABSTRACT: Systemic amyloidosis is a serious multiorgan disease with reduced life expectancy, irrespective of type. The impact of magnetic resonance imaging (MRI) in managing this condition has been immense. The last decade in particular has seen a surge of interest in the assessment and evaluation of the heart in patients with systemic amyloidosis by cardiovascular magnetic resonance imaging (CMR), with approximately 85% of all publications on this subject arising in the last 10 years. This has been largely driven by the creation of new sequences and their subsequent modernisation and technical development, thereby rendering previously prohibitive methods clinically more relevant and applicable. In turn, this has led to an increased awareness and recognition of the disease. This review demonstrates how MRI has become a pivotal diagnostic tool in the assessment of cardiac amyloidosis over the last 2 decades, with the ability to track disease and predict mortality. Several different pathognomonic patterns of late gadolinium enhancement (LGE) are now recognised and are able to prognosticate. T1 mapping and extracellular volume (ECV) techniques have resulted in even earlier disease detection before LGE is even visible and along with T2 mapping, provide new insights into biology. As newer therapies also evolve and become available, the need for accurate tracking of cardiac disease response to treatment carries increasing importance. All these are examined in this review, mainly focussing on light-chain (AL) and transthyretin (ATTR) amyloidosis.

KEYWORDS: Amyloidosis, Cardiac MRI, CMR, T1 mapping, T2 mapping, ECV, Late gadolinium enhancement, LGE

RECEIVED: January 19, 2019. **ACCEPTED:** March 19, 2019.

TYPE: Review

FUNDING: The author(s) received no financial support for the research, authorship, and/or publication of this article.

DECLARATION OF CONFLICTING INTERESTS: The author(s) declared no potential conflicts of interest with respect to the research, authorship, and/or publication of this article.

CORRESPONDING AUTHOR: Sanjay M Banypersad, Royal Blackburn Hospital, Haslingden Road, Blackburn BB2 3HH, UK. Email: sanjay.banypersad@elht.nhs.uk

Introduction

Magnetic resonance imaging has long provided excellent structural and functional information. The last decade in particular has seen a surge of interest in the assessment and evaluation of the heart in patients with systemic amyloidosis by cardiovascular magnetic resonance imaging (CMR), with approximately 85% of all publications on this subject arising in the last 10 years. This has been largely driven by the creation of new sequences and their subsequent modernisation and technical development, thereby rendering previously prohibitive methods clinically more relevant and applicable. This in turn has led to an increased awareness and recognition of the disease.

Long considered the archetypal extracellular disease process, systemic amyloidosis is a multisystem disorder characterised by infiltration of the interstitium of virtually any organ causing dysfunction. There are several types of systemic amyloidosis (see Table 1) but the commonest types affecting the heart are light-chain (AL) amyloidosis (typically caused by haematological malignancies) and transthyretin (ATTR) amyloidosis, the latter being further subdivided into (1) senile systemic amyloidosis (SSA), triggered by wild-type TTR produced in the liver; (2) variant ATTR amyloidosis, caused by point mutations in the TTR gene. Although the amyloid-forming precursor varies between AL and ATTR amyloidosis, the final common denominator is the same, ie, misfolding of proteins in the blood to form an insoluble β -pleated sheet, the signature of the amyloid fibril.¹

Cardiac amyloidosis exists when there is amyloid deposition in the heart of sufficient quantity to cause cardiac dysfunction.

Heart failure and arrhythmias are the commonest modes of presentation of cardiac amyloidosis. Cardiac AL amyloidosis is more aggressive than cardiac ATTR amyloidosis, the latter carrying a more benign disease course. Median survival is around 6 months without treatment in cardiac AL amyloidosis compared with several years in cardiac ATTR amyloidosis. Treatment is targeted towards eliminating the amyloid-forming precursor protein (i.e., halting progression) rather than towards the amyloid deposits themselves. In AL amyloidosis, chemotherapy eliminates the abnormal light chains or immunoglobulin precursor. Treatment of cardiac ATTR amyloidosis is governed by the subtype; in variant ATTR amyloidosis, liver transplantation can be curative by producing wild-type 'normal' TTR, while SSA can be palliated by transthyretin stabilising agents.¹ Eradication of amyloid deposits has been described in mouse models but is still in its experimental phase.²

The presence of cardiac amyloidosis portends a poorer prognosis across both AL and ATTR types, although this is undoubtedly worse in AL amyloidosis. Even with a successful complete haematological response, median survival is still only around 4 years, emphasising the paramount importance of detecting cardiac involvement as early as possible to improve outcome.¹

Before CMR was in widespread use, detecting cardiac involvement relied on suggestive ECG abnormalities in a patient with known AL amyloidosis elsewhere, or increased wall thickness on echo and raised NT-proBNP. None however specifically quantify amyloid burden and lack sensitivity and specificity. This review focuses on how MRI has consequently



Table 1. Showing the commonest types and subtypes of systemic amyloidosis.

AMYLOID TYPE	PRECURSOR PROTEIN	TYPICAL DECADE OF PRESENTATION	CARDIAC INVOLVEMENT	OTHER ORGAN INVOLVEMENT	TREATMENT	PROGNOSIS (MEDIAN SURVIVAL)
Primary (AL) amyloidosis	Monoclonal light chain	6th to 7th decade (but can be any)	50%-70%	Renal, liver, soft tissue, neuropathy	Chemotherapy or ASCT	48 months but 8 months for advanced stage disease
Transthyretin amyloidosis						
Senile systemic amyloidosis (SSA)	Wild-type TTR	70 years	Almost all cases	Carpal tunnel syndrome	Supportive	7-8 years
ATTR (V30M)	Variant TTR	3rd or 4th decade	Uncommon	Peripheral and autonomic neuropathy	Liver transplantation	Good with liver transplant for V30M
ATTR (T60A)	Variant TTR	6th decade	Up to 90% by diagnosis	Peripheral and autonomic neuropathy	Liver and heart transplant possible in selected patients	Variable with transplantation
ATTR Ile 122	Variant TTR	7th to 8th decade	Almost all cases	Carpal tunnel syndrome	Supportive	2-6 years
Apolipoprotein A1 (ApoA1)	Variant apolipoprotein	6th to 7th decade	Rare	Predominantly renal	Renal (+/- liver) transplant	Usually slowly progressive (years)
Secondary (AA) amyloidosis	Serum amyloid A (SAA)	Any	Rare	Renal, liver	Treat underlying condition	Good if underlying condition controlled
Atrial natriuretic peptide (ANP)	ANP	70 years or older	All cases (uncertain significance)	None reported	Not needed	—

become a pivotal diagnostic tool in the assessment of cardiac amyloidosis with the ability to track disease and predict mortality.

CMR in Context

Typically, a patient with suspected systemic amyloidosis undergoes a series of haematological, rheumatological, and renal investigations, with formal diagnosis resting on histological analysis of an affected organ (e.g., fat aspirate, rectal, bone marrow) stained with Congo Red and Immunohistochemistry. However, even though cardiac involvement is the principal driver of outcome, endomyocardial biopsy is seldom performed, mainly due to its invasive risks. Consequently, systemic amyloidosis *with cardiac involvement* is said to be present when peripheral tissue histology confirms AL amyloidosis and qualifying echocardiography parameters³ +/- serum biomarker permutations as designated in the Mayo classification, are also evident.⁴

Echocardiography is widely available and cost-effective. Left ventricular (LV) and right ventricular (RV) thickening are generally easily seen as infiltration by amyloid is said to contribute to a characteristic 'speckling' appearance. Diastolic dysfunction, typically an early sign of cardiac involvement, is best assessed by echocardiography compared with other imaging modalities, by virtue of tissue and transmitral Doppler measurements.

Nuclear scintigraphy plays an important role in systemic amyloidosis. Serum amyloid P (SAP) scintigraphy demonstrates amyloid uptake in visceral organs, primarily liver, kidneys, spleen, and adrenal glands. As it is radiolabelled SAP, it binds specifically to amyloid fibrils in organs and image intensity is directly proportional to amyloid burden. The historic bone tracer ^{99m}Tc-3,3-diphosphono-1,2-propanodicarboxylic acid (DPD) scintigraphy has found renewed importance in systemic amyloidosis. It binds to ATTR amyloid in the heart and the relative ratio of intensities of bone and cardiac uptake represents a qualitative measure of cardiac ATTR amyloid burden.

There are some challenges with these methods. Serum biomarkers are affected by co-existing renal/liver disease (causing ventricular distension due to fluid retention) and also change in response to specific chemotherapeutic agents.¹ SAP scintigraphy, while effective at demonstrating visceral organ uptake, does not image amyloid in the heart. Echocardiography does image the heart but is not specific for amyloidosis.

CMR provides superior spatial resolution to echocardiography thereby providing a gold standard, reproducible measure of radial and longitudinal systolic function. Cine imaging provides the first visual clues to the diagnosis of cardiac amyloidosis such as global LV and RV thickening, the patterns of which may be related to amyloid type.⁵ LV and left atrial ejection fraction can also be accurately determined.⁶ Cine imaging can also reveal associated alterations in systolic and diastolic

dysfunction measures by CMR,⁷ strain pattern,^{8,9} mitral and tricuspid annular plane systolic excursion¹⁰ and pericardial/pleural effusions, some of which are associated with adverse outcomes.¹¹

Late Gadolinium Enhancement Imaging

CMR can distinguish cardiac amyloidosis from other causes of left ventricular hypertrophy (LVH) such as hypertension and hypertrophic cardiomyopathy. Traditionally, the global subendocardial pattern of late gadolinium enhancement (LGE) has long been considered virtually diagnostic of the disease. In the 1990s, subendocardial LGE was shown to correlate with histology¹² but not with morbidity and mortality,¹³ somewhat unusual considering LGE generally portends worse outcomes in most disease states. Subsequent studies did little to clarify this, producing conflicting results regarding the prognostic utility of LGE imaging in amyloidosis.¹³⁻¹⁸ Current knowledge now offers several explanations for this.

First, the recognition that there is more than one characteristic pattern of amyloidosis (see Figure 1), which may have led to discrepancies in how LGE positivity using Magnitude only Inversion Recovery (MAG-IR) images was coded. The pattern of LGE can be atypical and patchy, especially in early disease.¹⁹ Effusions may cause considerable ghosting artefact, often a clue to the underlying diagnosis.^{12,13,20} Difficulties are frequently encountered with arrhythmias degrading image quality during CMR as well.

Second, the wider uptake of Phase Sensitive Inversion Recovery (PSIR) LGE imaging illustrated the difficulties in using MAG-IR techniques for LGE imaging in amyloidosis. LGE imaging is a thresholding technique; in amyloidosis, it is inherently challenging since amyloid infiltration within the interstitium of the heart reduces the differences in contrast signal between blood and myocardium such that the two compartments may null together or even be reversed, due to the very high uptake of gadolinium into the vastly expanded interstitia of severely amyloidotic hearts. When amyloid is diffusely and symmetrically deposited throughout the heart (i.e., not predominating in any particular region), myocardium may appear 'normal' (i.e., dark) on MAG-IR imaging, even though the entire myocardium is diseased (see Figure 2).

Furthermore, PSIR imaging acquires both phase and magnitude signal. As a result, amyloidotic tissue with the highest concentration of gadolinium will always appear bright. With MAG-IR imaging, however, because the myocardial and blood recovery curves crossover after the IR impulse in amyloidosis, nulled myocardium can be made to appear bright, simply by changing the operator setting of the inversion time (TI). In both patients in Figure 2, the MAG and PSIR images were acquired only a few seconds apart, but demonstrated opposite LGE patterns. The correct image is obtained when the TI is set greater than Y; the incorrect image is acquired if the TI is set at X. With PSIR imaging, the tissue with the least gadolinium

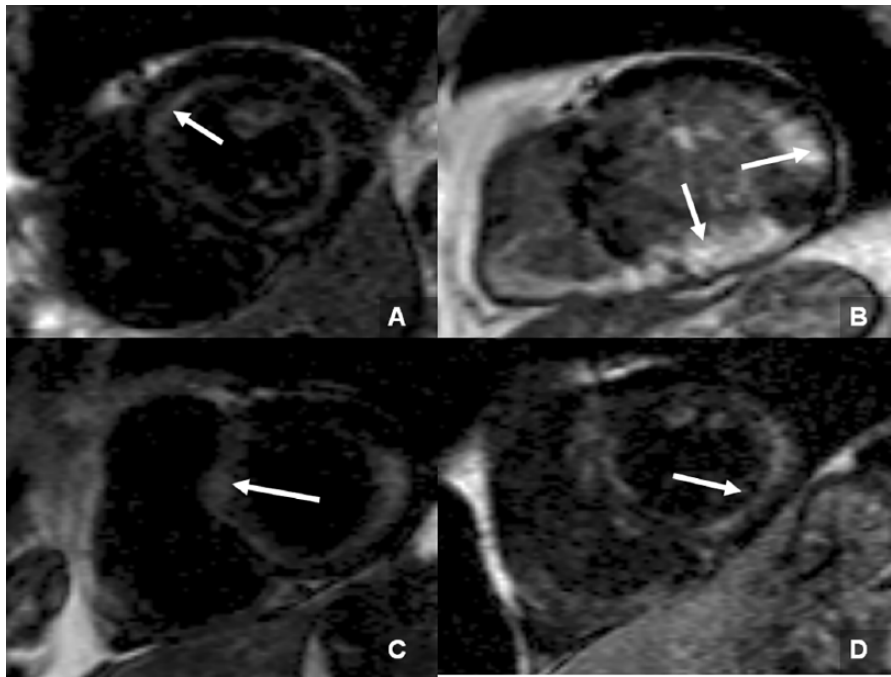


Figure 1. LGE patterns using MAG-IR imaging: (A) characteristic global, subendocardial; (B) patchy; (C) extensive; and (D) LGE in a patient without hypertrophy.²¹ MAG-IR indicates Magnitude only Inversion Recovery; PSIR, Phase Sensitive Inversion Recovery.

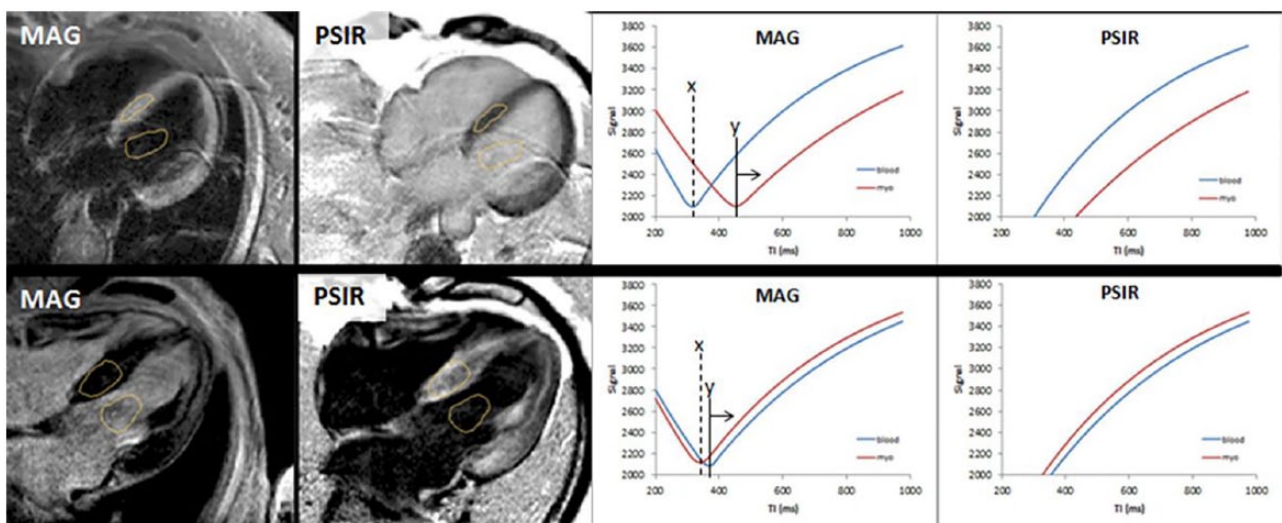


Figure 2. (Left) Two patients (top and bottom) with MAG-IR and PSIR LGE reconstruction images. (Right) Signal intensity curves as the T1 varies for MAG and PSIR.²²

has lower signal and is always nulled after windowing, irrespective of the T1 setting.

A recent, large CMR study of 250 amyloid patients confirmed that 100% of LGE areas obtained by PSIR imaging were correct compared with only 57% of MAG-IR images.²³ LGE presence predicted a universally worse outcome, with transmural LGE carrying higher mortality compared with subendocardial LGE.^{23–26} This was true for both cardiac AL and ATTR amyloidosis. The 2-year survival with no LGE was 92% in cardiac AL and ATTR amyloidosis, but this dropped to 81% with subendocardial LGE and dropped further still to 45% (AL) and 65% (ATTR) with transmural LGE.²²

RV LGE may also play a role in risk stratifying patients with cardiac amyloidosis.²⁷ So far, it has not been possible to reliably differentiate cardiac AL from ATTR amyloidosis based on LGE imaging alone; diagnostic scores have been designed in an attempt to address this, but have not met with widespread use.²⁸

T1 Mapping and Extracellular Volume

Key developments

Put simply, T1 represents the time taken for 63% of longitudinal magnetisation to recover after preparation by an inversion

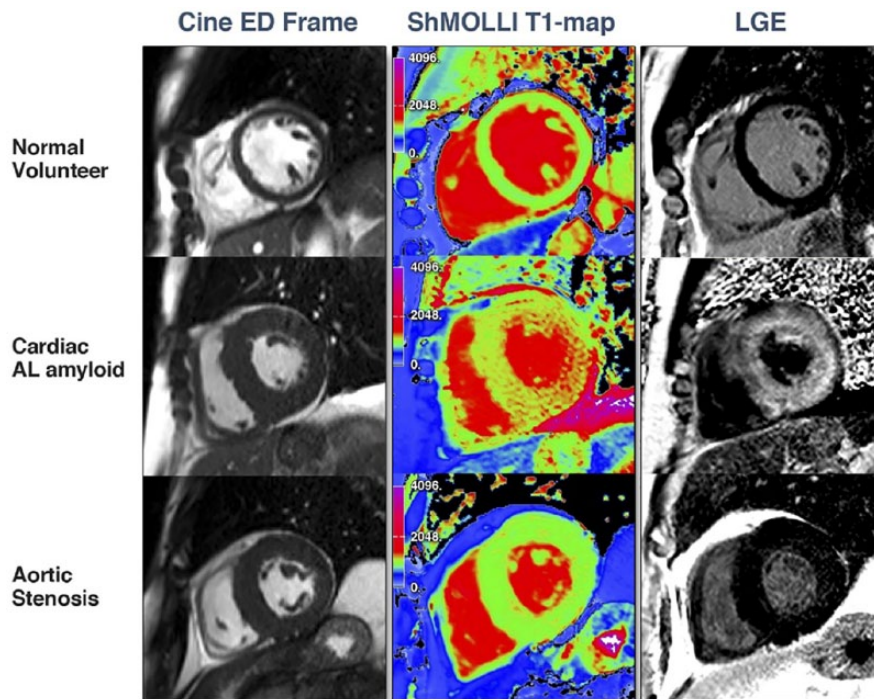


Figure 3. Cine still, ShMOLLI T1 map, and LGE image for (top) healthy volunteer; (bottom) cardiac AL amyloidosis patient (adapted from Karamitsos et al).³³ LGE indicates late gadolinium enhancement.

recovery impulse. It is a composite signal derived from cells and extracellular matrix. Tissues closest to water carry the highest T1 value (e.g., blood/cerebrospinal fluid) whereas tissues closest to solid state (e.g., fat/iron) have the lowest T1. The utility of T1 assessment in systemic amyloidosis had been noted as early as the 1980s but only in static extracardiac organs such as the liver,²⁹ because ECG gated sequences for myocardial assessment were not in widespread use—the Look-Locker sequence devised in the early 1970s only acquired myocardial T1 signal continuously throughout the cardiac cycle,³⁰ resulting in an inability to create a true pixel by pixel T1 map because of cardiac motion.

It was not until 2003, when the modified Look-Locker inversion recovery (MOLLI) sequence was devised, that full parametric T1 mapping of the myocardium became a reality.³¹ However, MOLLI still required multiple cardiac cycles in order that several data acquisitions could be merged to form a recovery curve for T1 estimation; this resulted in a prohibitively long breath-hold time for most patients with cardiac amyloidosis. Further modifications to shorten the MOLLI sequence (ShMOLLI)³² eventually made T1 mapping more clinically applicable while maintaining accuracy and reliability (see Figure 3). A region of interest can then be drawn in the myocardium to obtain the T1 value, which for normal myocardium is around 960 ± 30 ms on a 1.5T scanner.

Taking things a step further, as systemic amyloidosis is a purely extracellular disease process, quantification of only the extracellular volume (ECV) is a closer, non-invasive assessment of amyloid burden in the heart. ECV is calculated by

multiplying the non-cellular component of blood (i.e., the haematocrit) by the ratio of rate of change of myocardial T1: blood T1, obtained by T1 mapping; it also requires that the concentration of gadolinium in the blood plasma and interstitial space reach equilibrium. This was first achieved using the equilibrium CMR (Eq-CMR) technique to assess diffuse myocardial fibrosis in aortic stenosis and was validated against histology.³⁴

But although reproducible, there were limitations with this Eq-CMR technique. An infusion of gadolinium for half an hour with the need to take the patient in and out of the scanner hindered its clinical applicability. In addition, the use of multiple FLASH-IR sequences pre- and post-gadolinium and manually plotting curves to obtain T1 values made it clinically cumbersome. Subsequent technical developments by Fontana et al³⁵ and White et al³⁶ refined the ECV technique making it clinically more applicable by validating parametric T1 mapping and utilising only a single bolus of gadolinium with ECV calculations at 15 min post bolus.

Cardiac AL Amyloidosis

Extensive infiltration of the interstitium by amyloid matrix would be expected to increase native myocardial T1. Karamitsos et al³³ demonstrated in 53 AL amyloidosis patients that mean native myocardial T1 times measured by ShMOLLI were significantly raised (1140 ms) compared with the healthy volunteers (958 ms) with a cut-off value of 1020 ms having a diagnostic accuracy of 92% for cardiac amyloidosis. Higher values are observed on a 3T scanner.³⁷ Amyloidotic areas are

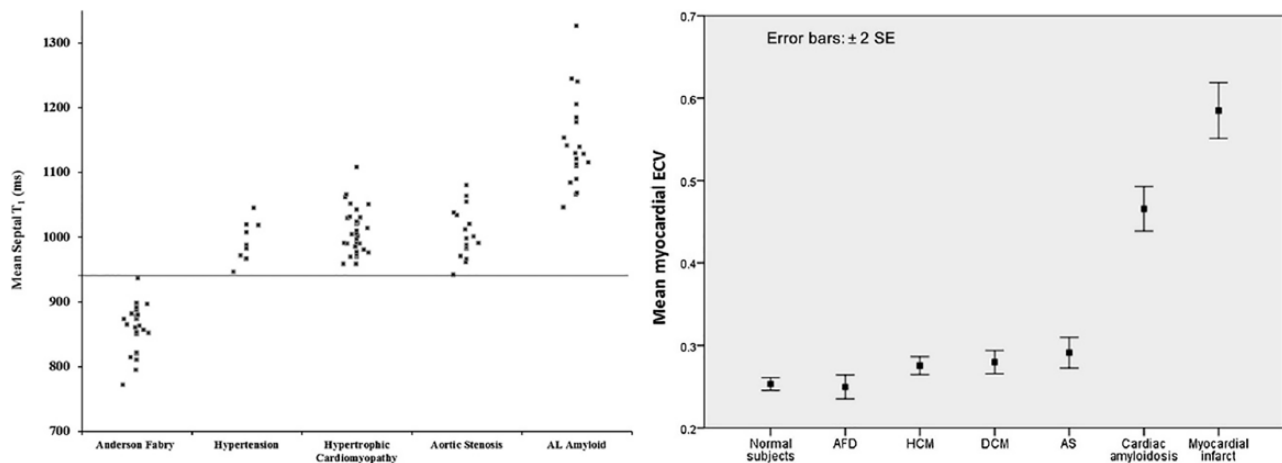


Figure 4. Comparison of (left) native myocardial T₁ and (right) Myocardial ECV, in various diseases presenting with left ventricular hypertrophy (adapted from Sado et al).³⁸ AFD indicates Anderson-Fabry disease; AS, aortic stenosis; DCM, dilated cardiomyopathy; HCM, hypertrophic cardiomyopathy.

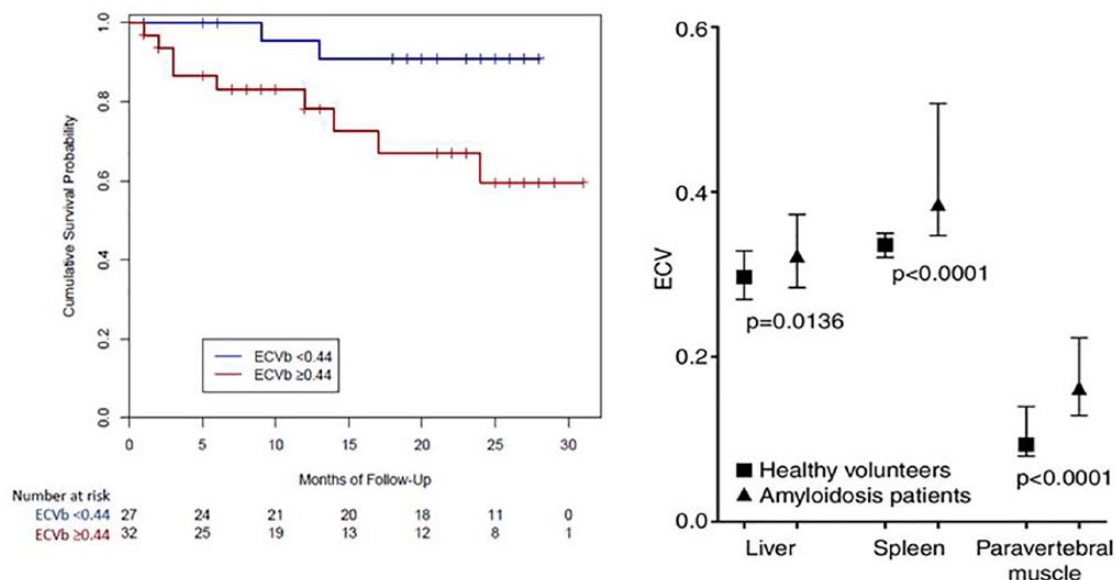


Figure 5. (Left) Survival curve for ECV (labelled ECVb here) in cardiac AL amyloidosis;⁴⁰ (Right) ECV in extracardiac organs in systemic AL amyloidosis compared with healthy volunteers.⁴² ECV indicates extracellular volume.

readily identified visually by the colour coded, higher T₁ signal (see Figure 3) which also tracked traditional markers of amyloid burden. Native myocardial T₁ was able to detect low grade disease based on pre-test probability scores but there was a degree of overlap with normality and high grade disease.

In a study of 60 patients with AL amyloidosis using the Eq-CMR technique, mean myocardial ECV was raised compared with healthy volunteers (0.44 vs 0.25) and demonstrated a tighter incremental correlation with probability of cardiac involvement based on echo and biomarker findings than native myocardial T₁.²¹ Multi-disease comparison studies show that ECV and T₁ reliably distinguish amyloidosis from other disease states (see Figure 4).^{38,39}

In a subsequent study of 100 AL amyloidosis patients followed up for a median duration of 2 years, a native myocardial T₁ of >1044ms and an ECV >0.45 predicted a higher mortality (see Figure 5), although only ECV is predictive on a 3T

scanner.³⁷ Because of the wide range of values in systemic amyloidosis compared with other diseases, ECV (and to a lesser extent, native T₁ mapping) can identify the presence of early cardiac disease (i.e., before LGE is present) in systemic AL amyloidosis,⁴⁰ thereby directing appropriate therapies with the likelihood of a better outcome and there is early evidence that ECV can demonstrate regression of myocardial amyloid after successful chemotherapy treatment.⁴¹

ECV is a robust measure that can also be applied to extracardiac organs and other conditions as well. In a study of 67 patients with systemic AL amyloidosis, ECV was significantly higher in the liver, spleen, and skeletal muscle in amyloidosis compared with healthy volunteers (see Figure 5) and additionally tracked conventional measures of hepatic and splenic amyloid burden by SAP scintigraphy.⁴² Incremental mortality of ECV has also been demonstrated in other conditions.^{43,44}

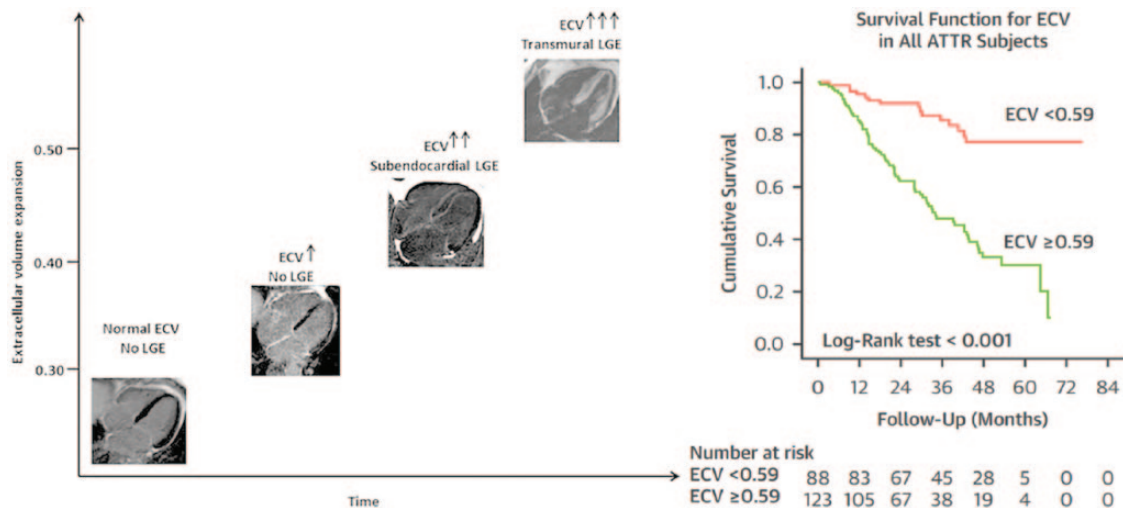


Figure 6. (Left) Amyloid 'cascade', showing progression from normal to advanced amyloid infiltration. (Right) Survival curve for ECV in cardiac ATTR amyloidosis.²² ECV indicates extracellular volume; LGE, late gadolinium enhancement.

Native T1 mapping has the advantage of not requiring gadolinium administration. But in a head-to-head comparison with ECV, the latter emerged the stronger predictor in comparative statistical models and also an independent predictor of mortality in multivariate analyses.⁴⁰ As described earlier, this is most likely explained by the fact that native T1 is a composite signal derived from cellular and extracellular relaxation times whereas ECV represents purely the extracellular expansion which, by inference, is the closest non-invasive quantifier of amyloid burden within the heart.

Cardiac ATTR Amyloidosis

Cardiac ATTR amyloidosis as mentioned earlier is divided into 2 main types. In African-Caribbean patients, ATTR amyloidosis is most commonly caused by a point mutation V122I in the TTR gene causing it to become amyloidogenic in the 7th to 8th decade life. In Caucasians, it is most commonly due to the wild-type TTR causing amyloid to form in the 7th or 8th decade of life (SSA), generally with a male preponderance. Unlike AL Amyloidosis, ^{99m}Tc-DPD scintigraphy is extremely useful in the detection of cardiac ATTR amyloidosis and classifying its extent.⁴⁵

In a study of around 200 patients with ATTR amyloidosis, ECV and native myocardial T1 behaved similarly AL amyloidosis in terms of diagnostic power. Both demonstrated incremental rises according to extent of amyloid infiltration although at high amyloid loads, native myocardial T1 did not correlate so well.⁴⁶ Both ECV and myocardial T1 correlated as a general trend with higher Perugini grades 0-3 on DPD scintigraphy, although no significant difference in ECV was seen between grades 2-3. As in AL amyloidosis, ECV and native myocardial T1 were able to detect early cardiac involvement (see Figure 6), with an intermediate range ECV of 0.3-0.4 showing some interstitial expansion when there is no LGE.^{22,47,48}

After a mean follow-up duration of 32 months, both ECV and native myocardial T1 predicted mortality with a hazard

ratio of approximately 1.2 for every 59 ms increase in T1 and for every 3% increase in ECV (see Figure 6). However, some interesting differences were also noted. ECV showed stronger correlations with systolic and diastolic function than native myocardial T1 and was also predictive of death when the SSA and variant ATTR groups were analysed separately whereas T1 was not. Furthermore, only ECV was independently predictive of mortality in a multivariate analysis whereas myocardial T1 was not predictive.⁴⁶

Native myocardial T1 values spanned a smaller range in ATTR compared with AL amyloidosis.^{22,47} By contrast, ECV values were generally higher in ATTR compared with AL amyloidosis. For the first time, these non-invasive markers provided a much needed insight into the pathophysiology in amyloidosis. ECV is derived from gadolinium movement between blood plasma and interstitium—since gadolinium is attracted to free water, ECV is telling us about differences in extracellular matrix composition between the 2 types and perhaps the changes which the matrix undergoes as the amyloid disease process develops.

Taking ECV a step further, performing $1 - (ECV \times LV \text{ mass})$ provides the mean cell volume which increased in ATTR as amyloid burden increased, but not in AL amyloidosis. This suggests that there is concomitant cell hypertrophy/hyperplasia (perhaps as high as 20%) in addition to the observed interstitial expansion in ATTR amyloidosis, something not seen in AL amyloidosis. It is postulated that this higher myocyte volume may explain the more benign natural history of cardiac ATTR compared with AL amyloidosis, where median survival is 38 vs 17 months, respectively. Further studies are required to confirm this theory.^{22,48}

T2 Mapping

High signal on T2 imaging of the heart represents myocardial oedema, typically seen in acute myocarditis, infarction, or inflammatory cardiomyopathies. Until recently, it had limited

use in amyloidosis because of conflicting results. Some studies have shown T2 ratio (T2 myocardium: T2 skeletal muscle) to be low in cardiac amyloidosis compared with healthy volunteers.^{49,50} But as patients with systemic amyloidosis frequently have deposits within skeletal muscle,⁴² this is likely to have been a confounder. Other studies have shown that T2 is no different in cardiac amyloidosis than normal.⁵¹ But these studies did not segregate AL from ATTR amyloidosis and small patient numbers may have underpowered these studies.

The most recent study of cardiac T2 mapping in 100 AL and 186 ATTR Amyloidosis patients overcame these limitations and showed a higher mean T2 of 56 and 54 ms, respectively, compared with 49 ms in healthy volunteers. A higher T2 was also associated with worse systolic function and correlated with demonstrable evidence of myocardial oedema on histological examination. After a follow-up period of approximately 2 years, myocardial T2 emerged as an independent predictor of prognosis in multivariate analysis after adjustment for ECV and serum biomarkers, with a T2 of >55 ms portending a 20% relative reduction in survival in cardiac AL amyloidosis; T2 was not predictive in ATTR amyloidosis.⁵²

This is likely because as stated earlier, data from T1 mapping studies in the last 5 years suggested that there is a failure of cell hypertrophy/hyperplasia in AL amyloidosis that must in some way explain its more aggressive clinical course and worse prognosis than ATTR amyloidosis.⁴⁸ In the most severe cases of cardiac AL amyloidosis, there is either an additional toxic effect of light chains (or perhaps the amyloid matrix itself) which contributes to cell death perhaps through a myocarditic process. This would explain the observation that T2 was not as high in treated (53 ms) compared with untreated (56 ms) cardiac AL amyloidosis.

Limitations of CMR

CMR is an expensive modality and is not available in all centres. It is not a portable technique like echocardiography and CMR scans, particularly involving T1 mapping, can still be long and time-consuming to perform and report. Some aspects of cardiac function cannot be assessed easily, such as diastology. LGE imaging is not specific to amyloidosis and while T1 mapping and ECV are a direct measure of interstitial expansion, their utilities in assessing treatment response and tracking disease progression through time still require validation.

Conclusions

Systemic amyloidosis is a serious multiorgan disease with reduced life expectancy, irrespective of type. The impact of MRI imaging in managing this condition has been immense. Several different pathognomonic patterns of LGE are now recognised and are able to prognosticate. T1 mapping and ECV have resulted in even earlier disease detection, before LGE is even visible. The increasing uptake of CMR in general has led to the detection of cardiac amyloidosis co-existing with other conditions such as severe aortic stenosis where it portends a

worse prognosis, thus impacting upon the decision-making process for these conditions.^{53,54}

CMR with native myocardial T1 and ECV have also provided new insights into biology. These techniques have brought us as close as we can be in the modern era to virtual histology such that with the sensitivity of DPD scintigraphy approaching virtually 100% in selected patients, the combination of CMR and DPD scintigraphy may be sufficient to avoid cardiac biopsy altogether.⁵⁵ However, the diagnostic performance of CMR compared with nuclear scintigraphy, particularly in the detection of early cardiac disease, has not yet been established.

It is no surprise therefore that the Society for Cardiovascular Magnetic Resonance and the European Association of Cardiovascular Imaging issued a Consensus Statement in 2017 recommending these sequences be used routinely in clinical practice,⁵⁶ especially considering that technical developments are continually refining various aspects of these parametric mapping sequences. A variety of T1 and ECV mapping sequences are now available.

New therapies for systemic amyloidosis are also in development. As mentioned earlier, the combination of (R)-1-[6-[(R)-2-carboxy-pyrrolidin-1-yl]-6-oxo-hexanoyl]pyrrolidine-2-carboxylic acid (known as CPHPC) with anti-SAP antibody was shown to eradicate amyloid deposits from the liver and spleen of mice.² For human studies, because SAP scintigraphy is not useful once anti-SAP has been administered, an alternative marker is required to non-invasively but nevertheless quantitatively measure amyloid burden before and after treatment. That ECV has proved a more powerful a predictor than native myocardial T1^{40,46} and can demonstrate disease regression^{41,57} has been a key factor in ECV becoming an endpoint in the phase 2 studies of this antibody trial.⁵⁸

There are of course still questions to answer: is there a myocarditic process in AL amyloidosis? Might myocyte loss in cardiac AL amyloidosis explains the low voltage ECGs more frequently encountered in AL compared with ATTR amyloidosis?^{1,59} T2 data needs multi-centre corroboration and we also need more robust methods of being able to correlate cardiac histology with ECV, T1, and T2 mapping data. Future work includes exploration of resting perfusion abnormalities known to occur in some cases of cardiac amyloidosis^{60,61} which are very likely to be important in risk stratification. And conclusive demonstration of amyloid regression coupled with proof that the new eradication therapies are safe and effective could prove a revolutionary combination to help end the scourge of this disease.

Author Contributions

SMB is the sole author of this article and therefore researched and wrote the entire article himself.

REFERENCES

1. Banypersad SM, Moon JC, Whelan C, Hawkins PN, Wechalekar AD. Updates in cardiac amyloidosis: a review. *J Am Heart Assoc.* 2012;1:e000364.

2. Bodin K, Ellmerich S, Kahan MC, et al. Antibodies to human serum amyloid P component eliminate visceral amyloid deposits. *Nature*. 2010;468:93–97.
3. Gertz MA, Comenzo R, Falk RH, et al. Definition of organ involvement and treatment response in immunoglobulin light chain amyloidosis (AL): a consensus opinion from the 10th international symposium on amyloid and amyloidosis, Tours, France, 18–22 April 2004. *Am J Hematol*. 2005;79:319–328.
4. Dispenzieri A, Gertz MA, Kyle RA, et al. Serum cardiac troponins and N-terminal pro-brain natriuretic peptide: a staging system for primary systemic amyloidosis. *J Clin Oncol*. 2004;22:3751–3757.
5. Martinez-Naharro A, Treibel TA, Abdel-Gadir A, et al. Magnetic resonance in transthyretin cardiac amyloidosis. *J Am Coll Cardiol*. 2017;70:466–477.
6. Mohty D, Boulogne C, Magne J, et al. Prognostic value of left atrial function in systemic light-chain amyloidosis: a cardiac magnetic resonance study. *Eur Heart J Cardiovasc Imaging*. 2016;17:961–969.
7. Kuetting DL, Homsi R, Sprinkart AM, et al. Quantitative assessment of systolic and diastolic function in patients with LGE negative systemic amyloidosis using CMR. *Int J Cardiol*. 2017;232:336–341.
8. Williams LK, Forero JF, Popovic ZB, et al. Patterns of CMR measured longitudinal strain and its association with late gadolinium enhancement in patients with cardiac amyloidosis and its mimics. *J Cardiovasc Magn Reson*. 2017;19:61.
9. Oda S, Utsunomiya D, Nakaura T, et al. Identification and assessment of cardiac amyloidosis by myocardial strain analysis of cardiac magnetic resonance imaging. *Circ J*. 2017;81:1014–1021.
10. Ochs MM, Fritz T, Arenja N, et al. Regional differences in prognostic value of cardiac valve plane displacement in systemic light-chain amyloidosis. *J Cardiovasc Magn Reson*. 2017;19:87.
11. Knight DS, Zumbo G, Barcella W, et al. Cardiac structural and functional consequences of amyloid deposition by cardiac magnetic resonance and echocardiography and their prognostic roles [published online ahead of print 18 April 2018]. *JACC Cardiovasc Imaging*. doi:10.1016/j.jcmg.2018.02.016.
12. Maccera AM, Joshi J, Prasad SK, et al. Cardiovascular magnetic resonance in cardiac amyloidosis. *Circulation*. 2005;111:186–193.
13. Maccera AM, Prasad SK, Hawkins PN, Roughton M, Pennell DJ. Cardiovascular magnetic resonance and prognosis in cardiac amyloidosis. *J Cardiovasc Magn Reson*. 2008;10:54.
14. Austin BA, Tang WH, Rodriguez ER, et al. Delayed hyper-enhancement magnetic resonance imaging provides incremental diagnostic and prognostic utility in suspected cardiac amyloidosis. *JACC Cardiovasc Imaging*. 2009;2:1369–1377.
15. Mekinian A, Lions C, Leleu X, et al. Prognosis assessment of cardiac involvement in systemic AL amyloidosis by magnetic resonance imaging. *Am J Med*. 2010;123:864–868.
16. Ruberg FL, Appelbaum E, Davidoff R, et al. Diagnostic and prognostic utility of cardiovascular magnetic resonance imaging in light-chain cardiac amyloidosis. *Am J Cardiol*. 2009;103:544–549.
17. Syed IS, Glockner JF, Feng D, et al. Role of cardiac magnetic resonance imaging in the detection of cardiac amyloidosis. *JACC Cardiovasc Imaging*. 2010;3:155–164.
18. Vogelsberg H, Mahrholdt H, Deluigi CC, et al. Cardiovascular magnetic resonance in clinically suspected cardiac amyloidosis: noninvasive imaging compared to endomyocardial biopsy. *J Am Coll Cardiol*. 2008;51:1022–1030.
19. Di Bella G, Minutoli F, Mazzeo A, et al. MRI of cardiac involvement in transthyretin familial amyloid polyneuropathy. *Am J Roentgenol*. 2010;195:W394–W399.
20. Sparrow PJ, Merchant N, Provost YL, Doyle DJ, Nguyen ET, Paul NS. CT and MR imaging findings in patients with acquired heart disease at risk for sudden cardiac death. *Radiographics*. 2009;29:805–823.
21. Banyersad SM, Sado DM, Flett AS, et al. Quantification of myocardial extracellular volume fraction in systemic AL amyloidosis: an equilibrium contrast cardiovascular magnetic resonance study. *Circ Cardiovasc Imaging*. 2013;6:34–39.
22. Fontana M, Pica S, Reant P, et al. Prognostic value of late gadolinium enhancement cardiovascular magnetic resonance in cardiac amyloidosis. *Circulation*. 2015;132:1570–1579.
23. Fontana M, Pica S, Reant P, et al. Response to letters regarding article, 'prognostic value of late gadolinium enhancement cardiovascular magnetic resonance in cardiac amyloidosis'. *Circulation*. 2016;133:e450–e451.
24. Baroni M, Nava S, Quattrocchi G, et al. Role of cardiovascular magnetic resonance in suspected cardiac amyloidosis: late gadolinium enhancement pattern as mortality predictor. *Netw Heart J*. 2018;26:34–40.
25. Raina S, Lensing SY, Nairouz RS, et al. Prognostic value of late gadolinium enhancement CMR in systemic amyloidosis. *JACC Cardiovasc Imaging*. 2016;9:1267–1277.
26. Boynton SJ, Geske JB, Dispenzieri A, et al. LGE provides incremental prognostic information over serum biomarkers in AL cardiac amyloidosis. *JACC Cardiovasc Imaging*. 2016;9:680–686.
27. Wan K, Sun J, Han Y, et al. Right ventricular involvement evaluated by cardiac magnetic resonance imaging predicts mortality in patients with light chain amyloidosis. *Heart Vessels*. 2018;33:170–179.
28. Dungu JN, Valencia O, Pinney JH, et al. CMR-based differentiation of AL and ATTR cardiac amyloidosis. *JACC Cardiovasc Imaging*. 2014;7:133–142.
29. Benson L, Hemmingsson A, Ericsson A, et al. Magnetic resonance imaging in primary amyloidosis. *Acta Radiologica*. 1987;28:13–15.
30. Look D, Locker DR. Time saving in measurement of NMR and EPR relaxation times. *Rev Sci Instrum*. 1970;41:250–251.
31. Messroghli DR, Radjenovic A, Kozierke S, Higgins DM, Sivananthan MU, Ridgway JP. Modified look-locker inversion recovery (MOLLI) for high-resolution T1 mapping of the heart. *Magn Reson Med*. 2004;52:141–146.
32. Piechnik SK, Ferreira VM, Dall'Armellina E, et al. Shortened modified look-locker inversion recovery (ShMOLLI) for clinical myocardial T1-mapping at 1.5 and 3 T within a 9 heartbeat breathhold. *J Cardiovasc Magn Reson*. 2010;12:69.
33. Karamitsos TD, Piechnik SK, Banyersad SM, et al. Noncontrast T1 mapping for the diagnosis of cardiac amyloidosis. *JACC Cardiovasc Imaging*. 2013;6:488–497.
34. Flett AS, Hayward MP, Ashworth MT, et al. Equilibrium contrast cardiovascular magnetic resonance for the measurement of diffuse myocardial fibrosis: preliminary validation in humans. *Circulation*. 2010;122:138–144.
35. Fontana M, White SK, Banyersad SM, et al. Comparison of T1 mapping techniques for ECV quantification. Histological validation and reproducibility of ShMOLLI versus multibreath-hold T1 quantification equilibrium contrast CMR. *J Cardiovasc Magn Reson*. 2012;14:88.
36. White SK, Sado DM, Fontana M, et al. T1 mapping for myocardial extracellular volume measurement by CMR: bolus only versus primed infusion technique. *JACC Cardiovasc Imaging*. 2013;6:955–962.
37. Lin L, Li X, Feng J, et al. The prognostic value of T1 mapping and late gadolinium enhancement cardiovascular magnetic resonance imaging in patients with light chain amyloidosis. *J Cardiovasc Magn Reson*. 2018;20:2.
38. Sado DM, Flett AS, Banyersad SM, et al. Cardiovascular magnetic resonance measurement of myocardial extracellular volume in health and disease. *Heart*. 2012;98:1436–1441.
39. Sado DM, White SK, Piechnik SK, et al. Identification and assessment of Anderson-Fabry disease by cardiovascular magnetic resonance noncontrast myocardial T1 mapping. *Circ Cardiovasc Imaging*. 2013;6:392–398.
40. Banyersad SM, Fontana M, Maestrini V, et al. T1 mapping and survival in systemic light-chain amyloidosis. *Eur Heart J*. 2015;36:244–251.
41. Martinez-Naharro A, Abdel-Gadir A, Treibel TA, et al. CMR-verified regression of cardiac AL amyloid after chemotherapy. *JACC Cardiovasc Imaging*. 2018;11:152–154.
42. Bandula S, Banyersad SM, Sado D, et al. Measurement of tissue interstitial volume in healthy patients and those with amyloidosis with equilibrium contrast-enhanced MR imaging. *Radiology*. 2013;268:858–864.
43. Wong TC, Piehler KM, Kang IA, et al. Myocardial extracellular volume fraction quantified by cardiovascular magnetic resonance is increased in diabetes and associated with mortality and incident heart failure admission. *Eur Heart J*. 2014;35:657–664.
44. Schelbert EB, Fridman Y, Wong TC, et al. Temporal relation between myocardial fibrosis and heart failure with preserved ejection fraction: association with baseline disease severity and subsequent outcome. *JAMA Cardiol*. 2017;2:995–1006.
45. Perugini E, Guidalotti PL, Salvi F, et al. Noninvasive etiologic diagnosis of cardiac amyloidosis using ^{99m}Tc-3,3-diphosphono-1,2-propanodicarboxylic acid scintigraphy. *J Am Coll Cardiol*. 2005;46:1076–1084.
46. Martinez-Naharro A, Kotecha T, Norrington K, et al. Native T1 and extracellular volume in transthyretin amyloidosis [published online ahead of print 14 March 2018]. *JACC Cardiovasc Imaging*. doi:10.1016/j.jcmg.2018.02.006.
47. Fontana M, Banyersad SM, Treibel TA, et al. Native T1 mapping in transthyretin amyloidosis. *JACC Cardiovasc Imaging*. 2014;7:157–165.
48. Fontana M, Banyersad SM, Treibel TA, et al. Differential myocyte responses in patients with cardiac transthyretin amyloidosis and light-chain amyloidosis: a cardiac MR imaging study. *Radiology*. 2015;277:388–397.
49. Wassmuth R, Abdel-Aty H, Bohl S, Schulz-Menger J. Prognostic impact of T2-weighted CMR imaging for cardiac amyloidosis. *Eur Radiol*. 2011;21:1643–1650.
50. Legou F, Tacher V, Damy T, et al. Usefulness of T2 ratio in the diagnosis and prognosis of cardiac amyloidosis using cardiac MR imaging. *Diagn Interv Imaging*. 2017;98:125–132.
51. Sparrow P, Amirabadi A, Sussman MS, Paul N, Merchant N. Quantitative assessment of myocardial T2 relaxation times in cardiac amyloidosis. *J Magn Reson Imaging*. 2009;30:942–946.
52. Kotecha T, Martinez-Naharro A, Treibel TA, et al. Myocardial edema and prognosis in amyloidosis. *J Am Coll Cardiol*. 2018;71:2919–2931.
53. Cavalcante JL, Rijal S, Abdelkarim I, et al. Cardiac amyloidosis is prevalent in older patients with aortic stenosis and carries worse prognosis. *J Cardiovasc Magn Reson*. 2017;19:98.
54. Treibel TA, Fontana M, Gilbertson JA, et al. Occult transthyretin cardiac amyloid in severe calcific aortic stenosis: prevalence and prognosis in patients undergoing surgical aortic valve replacement. *Circ Cardiovasc Imaging*. 2016;9:e005066.

55. Gillmore JD, Maurer MS, Falk RH, et al. Nonbiopsy diagnosis of cardiac transthyretin amyloidosis. *Circulation*. 2016;133:2404–2412.
56. Messroghli DR, Moon JC, Ferreira VM, et al. Clinical recommendations for cardiovascular magnetic resonance mapping of T1, T2, T2* and extracellular volume: a consensus statement by the Society for Cardiovascular Magnetic Resonance (SCMR) endorsed by the European Association for Cardiovascular Imaging (EACVI). *J Cardiovasc Magn Reson*. 2017;19:75.
57. Zumbo G, Barton SV, Thompson D, et al. Extracellular volume with bolus-only technique in amyloidosis patients: diagnostic accuracy, correlation with other clinical cardiac measures, and ability to track changes in amyloid load over time. *J Magn Reson Imaging*. 2018;47:1677–1684.
58. Richards DB, Cookson LM, Berges AC, et al. Therapeutic clearance of amyloid by antibodies to serum amyloid P component. *N Engl J Med*. 2015;373:1106–1114.
59. Maanja M, Wieslander B, Schlegel TT, et al. Diffuse myocardial fibrosis reduces electrocardiographic voltage measures of left ventricular hypertrophy independent of left ventricular mass. *J Am Heart Assoc*. 2017;6:e003795.
60. Martinez-Naharro A, Knight DS, Kotecha T, et al. Routine identification of hypoperfusion in cardiac amyloidosis by myocardial blood flow mapping. *Heart Vessels*. 2017;103:A24.
61. Li R, Yang ZG, Wen LY, et al. Regional myocardial microvascular dysfunction in cardiac amyloid light-chain amyloidosis: assessment with 3T cardiovascular magnetic resonance. *J Cardiovasc Magn Reson*. 2016;18:16.